Published in final edited form as:
Synapse. 2012 March ; 66(3): 204–219. doi:10.1002/syn.21502.

Immunohistochemical Localization of Enkephalin in the Human Striatum: A Postmortem Ultrastructural Study

Lesley A. McCollum[1,*], **Joy K. Roche**[2], and **Rosalinda C. Roberts**[2]

[1]Department of Neuroscience, University of Alabama at Birmingham, Birmingham, Alabama 35294 USA

[2]Department of Psychiatry and Behavioral Neurobiology, University of Alabama at Birmingham, Birmingham, Alabama 35294 USA

Abstract

Within the basal ganglia, the functionally defined region referred to as the striatum contains a subset of GABAergic medium spiny neurons expressing the neuropeptide enkephalin. Although the major features of ultrastructural enkephalin localization in striatum have been characterized among various species, its ultrastructural organization has never been studied in the human brain. Human striatal tissue was obtained from the Maryland and Alabama Brain Collections from 8 normal controls. The brains were received and fixed within 8 hours of death allowing for excellent preservation suitable for electron microscopy. Tissue from the dorsal striatum was processed for enkephalin immunoreactivity, and prepared for electron microscopy. General morphology of the dorsal striatum was consistent with light microscopy in human. The majority of neurons labeled with enkephalin were medium-sized, and had a large nonindented nucleus with a moderate amount of cytoplasm, characteristic of medium spiny neurons. Of the spines receiving synapses in dorsal striatum, 39% were labeled for enkephalin and were of varied morphologies. Small percentages (2%) of synapses were formed by labeled axon terminals. Most (82%) labeled terminals formed symmetric synapses. Enkephalin-labeled terminals showed no preference toward spines or dendrites for postsynaptic targets, whereas in rat and monkey, the vast majority of synapses in the neuropil are formed with dendritic shafts. Thus, there is an increase in the prevalence of axospinous synapses formed by enkephalin-labeled axon terminals in human compared to other species. Quantitative differences in synaptic features were also seen between the caudate nucleus and the putamen in the human tissue.

Keywords

Caudate; putamen; electron microscopy; neuroanatomy; synapse

INTRODUCTION

The striatum, a functionally defined region within the basal ganglia, is implicated in motor, cognitive, and behavioral functions (Beach and McGeer, 1984; Haber, 1986; Parent and Hazrati, 1995). It is responsible for the integration of glutamatergic cortical and thalamic inputs to the basal ganglia (Alexander et al., 1986, 1990), as well as dopaminergic inputs from the substantia nigra and ventral tegmental area (Björklund and Dunnett, 2007). Additionally, there are two output pathways of the basal ganglia, the indirect and direct pathways which originate from GABAergic medium spiny neurons containing either

[*]Correspondence to: Lesley A. McCollum, University of Alabama at Birmingham, 841 Sparks Center, 1530 3rd Ave South, Birmingham, AL 35294. Phone: 205-994-1968 Fax: 205-996-9377 lbryant@uab.edu.

enkephalin or substance P, and project to the external globus pallidus or internal globus pallidus/substantia nigra pars reticulata, respectively (Gerfen et al., 1991, 1992; Parent and Hazrati, 1995; Smith et al., 1998; Tepper et al., 2007). Dopamine projections from the substantia nigra differentially regulate these pathways through specific types of dopamine receptors (D_1 and D_2) found on the postsynaptic targets (Gerfen et al., 1990; Kubota et al., 1986; Parent and Hazrati, 1995).

Enkephalin, a pentapeptide that targets delta opioid receptors (Hughes et al., 1975), colocalizes with dopamine D_2 receptors in medium spiny projection neurons forming the indirect pathway (Aubert et al., 2000; Gerfen et al., 1990; Gerfen, 1992; Parent and Hazrati, 1995). These enkephalinergic neurons also send local collaterals to medium spiny neurons of the direct and indirect pathways (Parent and Hazrati, 1995; Yung et al., 1996), as well as to cholinergic interneurons (DiFiglia et al., 1982; Martone et al., 1992). Enkephalin has been shown to have neurotransmitter-like properties in striatum by studies showing potassium-induced release (Henderson et al., 1978) and the localization of enkephalin in fibers and terminals in association with opiate binding sites (Elde et al., 1976; Kuhar, 1978; Pasternak et al., 1975; Simantov et al., 1977). The endogenous ligand provides inhibitory modulation of neurons through opiate receptors (Frederickson and Norris, 1976; Hughes et al., 1975; Miller and Pickel, 1980).

Heterogeneous staining of enkephalin has been observed in cell bodies, fibers, and terminals of rodent (Ingham et al., 1991; Penny et al., 1986; Pickel et al., 1980; Sar et al., 1978; Somogyi et al., 1982), cat (Beckstead and Kersey, 1985; Penny et al., 1986), and primate striatum (DiFiglia et al., 1982; Haber and Elde, 1982; Ingaki and Parent, 1985; Martin et al., 1991) using light microscopy. Enkephalin staining exhibits an increasing dorsoventral gradient pattern in striatum, with denser enkephalin immunoreactivity in ventral areas (Beckstead and Kersey, 1985; Holt et al., 1997; Miller and Pickel, 1980; Somogyi et al., 1982). Neurons demonstrating enkephalin immunoreactivity comprise 49% of the neurons in monkey caudate nucleus (DiFiglia et al., 1982), and 38-47% in cat striatum (Penny et al., 1986). The enkephalin immuno-positive cell bodies observed in rat, cat, and monkey striatum are medium-sized (Beckstead and Kersey, 1985; DiFiglia et al., 1982; Hökfelt et al., 1977; Sar et al., 1978). These labeled cells correspond to spiny type I neurons or aspiny type I neurons (DiFiglia et al., 1976), which are the projection neurons and some of the local interneurons, respectively, that make up the striatum.

Synaptic organization of enkephalin has been characterized at the electron microscope level in rodents and non-human primates. Enkephalin immuno-positive neurons with large nonindented nuclei and scant cytoplasm have been observed in rat and monkey striatum (DiFiglia et al., 1982; Pickel et al., 1980), and are characteristic of spiny type I neurons (DiFiglia et al., 1976). In both species, synapses formed by enkephalin-labeled boutons are primarily symmetric onto unlabeled cell bodies, proximal dendrites, distal dendrite shafts, and axon initial segments. Enkephalin-labeled terminals forming asymmetric synapses onto spines are occasionally present in monkey (DiFiglia et al., 1982), but rarely in rat (Ingham et al., 1991; Roberts and Lapidus, 2005; Somogyi et al., 1982).

Although the major features of enkephalin localization at the ultrastructural level have been characterized among various species, the ultrastructural organization of enkephalin has never been studied in the human striatum. Thus, this study is aimed at the continuing characterization of the striatum in normal human brain. Some of this work has been published in preliminary form (Bryant et al., 2010).

MATERIALS AND METHODS

Human brain tissue

Postmortem human brain tissue was obtained from the Alabama Brain Collection (IRB# F080306003) and Maryland Brain Collection (IRB# HP-00043632), with consent from the next of kin (Table I). In addition, we have non-human subjects protocols for tissue from the Maryland Brain Collection that is used at UAB (N110411002 and N110411003). The tissue was collected from eight adult control subjects (5 males, 3 females) ranging in age from 32 to 68 years, with no history of central nervous system disease or neurological disease as determined by family interviews, autopsy reports (if applicable) and gross neuropathology reports. The mean ± SD for age, postmortem interval, and pH were 50.6 ± 14.3 years, 6.3 ± 1.6 hours and 6.7 ± 0.4, respectively (see Table I for individual case data). The brains were kept on ice until coronal blocks (1 cm thick) were cut and immersed in fixative within 8 hours of death. For the present study, coronal blocks of the striatum were immersed in a cold solution of 4% paraformaldehyde and 1% gluteraldehyde in 0.1 M phosphate buffer (pH 7.4; PB) for electron microscopy, pH 7.2-7.4, for a period of at least 1 week (4°C). Paraformaldehyde-glutaraldehyde fixation followed by sodium borohydride treatment (see Immunohistochemistry section of Materials and Methods) has been shown to be an optimal technique for ultrastructural immunohistochemistry as it preserves tissue ultrastructure and maintains antigenicity. Tissue samples were taken from the head of the caudate nucleus and anterior putamen.

Immunohistochemistry

The tissue was cut at a thickness of 40 μm with a Vibratome (HM 650V, Microm), and free-floating sections of one series out of six were processed for the immunohistochemical localization of enkephalin.

Immunohistochemistry was carried out using a polyclonal rabbit antiserum raised against synthetic Leucine Enkephalin conjugated to keyhole limpet hemocyanin (Incstar, #20066). Leucine (Leu)-enkephalin, with sequence Tyr-Gly-Gly-Phe-Leu, is a pentapeptide derived from the precursor protein preproenkephalin.

Briefly, the sections were collected in cold 0.1 M PB for 5 minutes, incubated at room temperature (RT) in a 1% sodium borohydride in PB for 15 minutes and rinsed four times for 5 minutes each in PB. Treatment with sodium borohydride is widely used for the unmasking of antigens, particularly in gluteraldehyde fixed tissue, by reduction of aldehyde linkages. The sections were then preincubated at RT in 10% normal goat serum in 0.01 M PB for 30 minutes, and subsequently incubated at 4°C in rabbit anti-Leu-enkephalin (1:2,000; Incstar) in a solution of 3% normal goat serum in 0.01 M PB for 72 hours. After four 5-minute rinses in PB, the sections were incubated at RT in biotinylated goat anti-rabbit IgG (1:200, Vector Laboratories) in a solution of 1.5% normal goat serum in 0.01 M PB for 45 minutes, and rinsed four times for 5 minutes each in PB. The sections were then incubated for 45 minutes at RT with the avidin-biotin complex (ABC standard kit, Vector Laboratories) based on methods of Hsu et al. (1981), and rinsed four times for 5 minutes each in PB. To visualize the reaction product, sections were incubated in 3, 3'-diaminobenzidine (10 mg diaminobenzidine, 15 ml PB, 12μL 0.03% hydrogen peroxide; Vector Laboratories, SK-4100) for 2-7 minutes. All washes and incubations were done under continuous agitation.

The precursor for leu-enkephalin, preproenkephalin, also gives rise to the highly similar pentapeptide methionine (met)-enkephalin (Tyr-Gly-Gly-Phe-Met). Due to the similarity of the two pentapeptide sequences, the anti-leu-enkephalin primary antibody used in this study invariably crossreacts with met-enkephalin. However, this will not confound the results for

its distribution since met-enkephalin and leu-enkephalin come from the same precursor and thus are in the same neurons. Additionally, the proenkephalin precursor contains 4 copies of met-enkephalin and a single copy of leu-enkephalin, so it would be expected that anti-leu-enkephalin crossreactivity with met-enkephalin would aid the ability to detect enkephalinergic structures. Characterization of the anti-leu-enkephalin primary antibody used in this study has been previously published. It is shown to give patterns of immunolabeling comparable to the same or other antibodies for enkephalin (Tripathi et al., 2010). Specificity of the primary antibody has been confirmed by pretreatment with 50 μg of leu-enkephalin per mL of diluted antiserum which completely eliminated staining (Tripathi et al., 2010). Pretreatment with 50 μg of met-enkephalin per mL of diluted antiserum also significantly blocks staining (manufacturer's data sheet). Specificity of the secondary antiserum was verified by omitting the primary antibody, but otherwise performing an identical protocol. When the primary antibody was omitted, no staining was present.

Light Microscopy

Tissue to be observed at the light microscopic level was dehydrated in increasing concentrations of EtOH, followed by xylene. The sections were mounted onto glass slides and coverslipped with Eukitt. Light micrographs were taken at a magnification of 40X on a Nikon Eclipse 50*i* microscope connected to a Nikon DS-Fi1 color digital camera.

Electron Microscopy

Sections from the dorsal striatum only (not including the ventral striatum) of both the caudate nucleus and the putamen were processed for electron microscopic analysis using standard techniques. Tissue samples 0.5 × 1.0 cm were excised from the caudate nucleus and putamen from each subject and flat embedded separately. Briefly, the sections were rinsed two times in 0.1 M PB for 5 minutes each, immersed in 1% osmium tetroxide in 0.1 M PB at RT, in the dark, for 1 hour, rinsed four times for 5 minutes each, then dehydrated in the dark, at RT, in increasing concentrations of EtOH. Following dehydrations, the tissue was stained en bloc in a 1% uranyl acetate solution in 70% EtOH for 1 hour for contrast, then rinsed in 70% EtOH two times for 5 minutes each. The tissue was dehydrated in increasing concentrations of EtOH, followed by 100% propylene oxide, then embedded in resins, and heated at 60°C for 72 hours. Areas of optimal staining from the caudate nucleus and putamen of all eight subjects were blocked. For quantitative analyses, 2-3 sections per case, at least 240 μm apart, were thin-sectioned. Serial ultrathin sections (90 nm thick) were collected using a Leica EM UC6 ultramicrotome. Serial sections were mounted on formvar-coated copper grids and photographed at 80 kV on a Hitachi 87650 transmission electron microscope using a Hamamatsu ORCA-HR digital camera. Electron micrographs were taken in regions containing optimal enkephalin staining. Neurons were photographed at a magnification of 5,000X. Neuropil was photographed at a magnification of 15,000X from ribbons of 8 to 14 serial sections. In order to photograph a large field of neuropil, four-by-two montages of individual overlapping digital micrographs were taken and stitched together using PanaVue ImageAssembler 3.

Data Collection and Analysis

Qualitative analyses were done from the dorsal caudate nucleus and putamen in all eight subjects. Quantitative analyses consisted of unbiased stereology counts and simple profile counts in five of the subjects (indicated in Table I) with the best ultrastructural preservation and immunoreactivity. Data from all five subjects were combined for proportional data, and averaged for density data. To determine the density of synapses in the neuropil, serial sections were analyzed using the disector technique (Geinisman et al., 1996; Sterio, 1984) as described in Perez-Costas et al. (2007). This 3-dimensional technique ensures that all parts

of the region are sampled and that all synapses within the region have equal probability of being sampled, providing an unbiased estimate of the total number of synapses. Since tissue received for this study from the Maryland Brain Collection did not contain the entire striatum, we were unable to measure the entire volume of the striatum to determine total synapse numbers. Thus, our results are given as densities as well as proportions determined by the stereology approach discussed above. All synapses in this study were identified by the first and last author using Adobe Photoshop at 50% zoom. Micrographs were cropped and adjusted for brightness and contrast in Adobe Photoshop to achieve optimal demarcation of the ultrastructure for presentation in the figures.

Criteria for distinguishing a synapse were the presence of (1) parallel pre- and postsynaptic membranes, (2) a postsynaptic density, and (3) synaptic vesicles at the membrane in the presynaptic terminal. All three criteria had to be fulfilled for the synapse to be counted. Stereology was used to determine the proportion of labeled and unlabeled terminals forming synapses, as well as the proportion of labeled versus unlabeled spines. Several synaptic features were quantified, including symmetry (asymmetric or symmetric) based on the morphology of the postsynaptic density, and the postsynaptic target (dendrite shaft or dendritic spine). Using stereology, a total of 1,138 synapses were counted in 8,355 μm^3 of striatum. Because the number of labeled terminals identified using stereology was small (n=49), simple profile counts (SPC) consisting of 2-dimensional random sampling of labeled boutons were also performed using the three criteria listed above. Over 90 sections were observed at 20,000X covering a large area for simple profile counts, and a total area of approximately 6,500 μm^2 containing potential labeled terminals was photographed at 25,000X for analysis. A total of 39 boutons were identified and quantified to determine the proportion of labeled terminals forming synapses (1) with spines versus dendrites, (2) that were asymmetric versus symmetric, and (3) with labeled versus unlabeled profiles. Finally, stereology was used to quantify the density and proportions of synapses with perforated postsynaptic densities ending on labeled versus unlabeled spines. These synapses were identified by a perforation in the postsynaptic density greater than the width of two synaptic vesicles (Geinisman et al., 1986a,b, 1988, 1989). Synapses with perforated postsynaptic densities will hereafter be referred to as perforated synapses for brevity. Data for neurons were collected using simple profile counts in single sections. The total number of neurons studied was 85 (50, putamen; 35, caudate).

Statistical analyses were used to verify the observed trends. The p-values reported for proportional results are from chi-square analyses or Fisher's exact test on the combined case data, while p-values reported for density data were calculated using a Wilcoxon Signed Rank test. No statistically significant differences were found when subjects were grouped by sex and analyzed using a Mann-Whitney test for the caudate or the putamen, however it is important to keep in mind the small sample sizes before ruling out sex differences.

RESULTS

At the light microscopic level, enkephalin labeling was seen in cell bodies and fibers throughout the striatum (Fig. 1). Cellular and synaptic localization of enkephalin immunoreactivity was quantified in the caudate nucleus and the putamen of normal human tissue using stereology. Simple profile counts were used in addition to stereology for the localization of enkephalin in axon terminals. Montages covering a large field of neuropil and taken from serial sections were used for stereology (Fig. 2). They were viewed at a higher magnification to quantify profiles within the neuropil (Fig. 3). Results of the quantitative analysis of labeled profiles are summarized as proportions in Table II. To find proportions for the two regions, n values were summed across individuals. Due to the nature of human

tissue however, there was some interindividual variability. The variability of profile densities of only the salient points are shown in Table III.

The majority of the enkephalin-positive striatal neurons observed in this study were medium-sized and characterized by a large nonindented nucleus and a moderate amount of cytoplasm (Fig. 4A). Some of the neurons (3/85) showed an indentation or notch in the nucleus, but were otherwise similar. Organelles present in labeled cell bodies include mitochondria, rough endoplasmic reticulum, polyribosomes, lysosomes, and occasionally (11% of cells) the Golgi apparatus. An average of 8 lysosomal bodies was present in each soma. Additionally, a perisomatic glial cell had adjacent membranes with 39% of the labeled neurons. Enkephalin-like immunoreactivity was diffuse throughout the cytoplasm of cell bodies and dendrites, localized primarily on polyribosomes and was also present on rough endoplasmic reticulum. Cell nuclei of neurons were also positive for enkephalin, with markedly lighter staining than that of the surrounding perikarya, with immunoreactivity localized in small clusters on euchromatin.

Labeled postsynaptic profiles were abundant throughout the caudate nucleus and putamen and received asymmetric and symmetric synapses. Labeled dendrite shafts and dendritic spines of various shapes were postsynaptic to terminals. The morphology of enkephalin-labeled spines included long necks with elongated heads (Fig. 3), thin necks with large heads (Fig. 4B), wide necks with large heads (Fig. 4D), thin necks with small heads (Fig. 4E), mushroom shaped (Fig. 4F), and spines with spinules (Fig. 4C). Labeled spines receiving synapses had similar densities in both regions (Fig. 5) however, a smaller density of total spines (labeled and unlabeled) receiving synapses in the putamen results in a significant difference in the proportions of labeled spines between the two regions; 32% of spines in the caudate nucleus and 44% of spines in putamen contained enkephalin immunoreactivity ($p<0.001$, $n=1680$).

Synapses with perforated postsynaptic densities were formed with spines (91%) and occasionally with dendrites (9%; Fig. 4C,F). Using stereology, the caudate nucleus and putamen had similar densities of perforated synapses (Fig. 5). Perforated synapses on labeled spines had similar densities in the two regions (Fig. 5), however the proportions were somewhat uneven. In the putamen, perforated synapses targeted a slightly higher proportion of labeled spines (59%) than unlabeled spines (41%), while in the caudate nucleus, spines receiving perforated synapses were labeled 47% of the time. The difference in the proportions of perforated synapses targeting labeled versus unlabeled spines was significantly different ($p=0.02$, $n=405$) between the putamen and the caudate nucleus. All dendrites receiving perforated synapses in the putamen were immuno-positive, but perforated synapses showed no preference for immuno-positive versus immuno-negative dendrites in the caudate nucleus.

Both myelinated and unmyelinated axons revealed enkephalin immunoreactivity (Fig. 7). Axon terminals containing immunoreactivity varied in size, but were usually small, and typically had round, clear synaptic vesicles with reaction product deposited around the vesicles (Fig. 7). Large dense core vesicles not associated with the synapse were also present in some terminals. Using stereology, synapses formed by labeled axon terminals were very infrequent (1.1% and 4.3% of all synapses in the putamen and the caudate nucleus, respectively). The densities of synapses formed by labeled terminals (Fig. 8) were not significantly different between the caudate and the putamen ($p=0.08$, $n=5$). Many labeled axon terminals observed in multiple planes of section never made contact with a postsynaptic target (Fig. 4E), or made contact but failed to fulfill all three synaptic criteria (not shown). Labeled axon terminals forming synapses that met all three synaptic criteria terminated on cell bodies (Fig. 6), dendrites (Fig. 7E,G-H), and spines (Fig. 7B-D,F). They

typically had symmetric postsynaptic membrane specializations (82% in the caudate and putamen combined), and primarily formed synapses with unlabeled profiles (86% in the caudate and putamen combined). The density of labeled terminals forming symmetric synapses was significantly (p=0.043, n=5) higher in the caudate than in the putamen (Fig. 8). Labeled terminals forming asymmetric synapses were occasionally identified in both regions. They had similar densities in the caudate nucleus and putamen (Fig. 8) but asymmetric synapses comprised a significantly (p=0.029, n=49) larger proportion of the synapses formed by labeled terminals in the putamen (42%) than in the caudate nucleus (11%). Using stereology, labeled axon terminals tended to form more synapses with spines rather than dendrites (58% vs. 42%) in putamen, while no difference was observed in the caudate nucleus (49% vs. 51%); these differences were not statistically significant (p=0.74, n=49). Enkephalin-labeled terminals forming asymmetric synapses with spines tended to synapse on the spine head, whereas those forming symmetric synapses with spines tended to synapse on either the spine neck or head. The labeled terminals forming symmetric synapses onto spine heads often synapsed on spines receiving convergent input from an unlabeled terminal forming an asymmetric synapse. Labeled axon terminals forming synapses on cell bodies were often long with multiple contact points (Fig. 6C-G). Similar results were found with simple profile counts (Table II).

DISCUSSION

Synaptic localization of enkephalin has previously been characterized in rodent and non-human primate striatum (DiFiglia et al., 1982; Ingham et al., 1991; Pickel et al., 1980; Somogyi et al., 1982), however in humans, striatal enkephalin labeling has only been observed at the light microscopic level (Holt et al., 1997; Prensa et al., 1999). Quantitative ultrastructural analyses of human postmortem brain are rare outside of our laboratory, due in part to the difficulty in obtaining brains with very short postmortem intervals. To our knowledge, this is the first time the ultrastructural localization of enkephalin has been studied in human striatum. The major findings in the present study include differences between the human striatum and that of other species (Table IV), as well as differences between the caudate nucleus and putamen of the human striatum. The major difference found between species was an increase in labeled axospinous synapses in humans compared to rodents and non-human primates. Within the human striatum, differences in enkephalin staining patterns are seen between the caudate nucleus and the putamen. The major findings include more local collaterals of enkephalin neurons in the caudate nucleus, and a larger proportion of labeled spines receiving perforated synapses in the putamen. The striatum has traditionally been considered a single entity; functional differences have been identified but largely attributed to the differences in connections with other brain areas. The present study reveals cytological differences between the caudate nucleus and the putamen in normal human tissue with detailed quantitative analyses. Variability between individual cases is shown in Table III, which also summarizes some of the differences found between the two regions in the human striatum.

Limitations and Technical Caveats

Some technical caveats must be considered with the interpretation of these data. For the quantification of labeled axon terminals in the present study, two techniques were used due to the rarity of axon terminals containing enkephalin immunoreactivity: stereology and simple profile counts. These techniques allowed us to look for trends using larger sample sizes, as conclusions could then be drawn from the simple profile count data in conjunction with the stereology data. Thus, the method of using simple profile counts in addition to stereology was not for the purpose of comparing between the techniques, but to gain a larger n for quantifications, and has been used in previously published ultrastructural studies in

human striatum (Hutcherson and Roberts, 2005; Kung et al., 1998). The simple profile count data agree with the results from stereology (Table II).

A limitation due to the use of human tissue in this study does not allow us to determine total synapse numbers (discussed in methods). This provides important implications for the use of these data in future studies of human striatum for disease states where the striatal volume may be altered, which would result in ambiguity when comparing densities. Thus, total synapse numbers would first need to be determined in the control human tissue to allow for an adequate comparison between the control and disease states.

Because similar trends were found with the simple profile counts and stereology techniques, and the general morphology of the striatum in the present study is consistent with our previous electron microscopy studies on control human tissue and that of other species (DiFiglia et al., 1982; Hutcherson and Roberts, 2005; Kemp and Powell, 1971b; Kung et al., 1998; Parent and Hazrati, 1995; Pasik et al., 1976; Somogyi et al., 1982), we can infer that any disagreement of the present study with published reports on other species is likely to result from a species difference rather than a methodological difference.

Variations in enkephalin immunoreactivity distribution occur in striosome versus matrix components of cat, monkey, and human striatum (Graybiel et al., 1981; Groves et al., 1988; Haber and Elde, 1982; Holt et al., 1997; Ingaki and Parent, 1985; Martin et al., 1991; Prensa et al., 1999); rings of dense enkephalin immunoreactivity with enkephalin-poor centers correspond to striosomes which are surrounded by relatively low levels of staining in the matrix in human striatum (Holt et al., 1997; Prensa et al., 1999). It is important to note that the distribution of enkephalin in striosome and matrix compartments was not examined in this study. Scientifically, we wanted to make as direct of a comparison as possible to the work done in previous species at the electron microscopic level, and striosomes were not taken into consideration in the past electron microscopy studies of enkephalin distribution. Methodologically, the tissue had to be cut with a vibratome for electron microscopy, which results in a more homogeneous pattern of labeling that differs from that of tissue prepared for light microscopy using conventional methods (i.e. with a freezing microtome and triton). Variation in synaptic organization of the striosomes and matrix has been reported in humans (Roberts and Knickman, 2002), thus different methods which allow for an examination of ultrastructural localization of enkephalin in striosomes versus matrix in humans will probably reveal a more complicated pattern of synaptic organization than was observed in the present study. This aspect of enkephalin distribution will be an important extension of the present study.

Labeled Neurons

Light microscopy studies in human striatum have previously shown that enkephalin immunoreactivity exhibits a gradient pattern of increasing staining from dorsal to ventral striatum (Holt et al., 1997). The results of the present study are consistent with the light microscopy studies in human as well as in rat striatum (Pickel et al., 1980; Somogyi et al., 1982), showing trends of more labeled profiles in ventral areas than dorsal. Neurons in human striatum exhibited low intensity reaction product throughout the cytoplasm of the cell body and dendrites, as well as light staining within the nucleus, consistent with reports in rat and monkey (DiFiglia et al., 1982; Pickel et al., 1980). Enkephalin-labeled cells were most often identified by a medium-sized soma, a large nonindented nucleus and a moderate amount of cytoplasm, morphological features corresponding to medium spiny projection neurons (Kemp and Powell, 1971a; Parent and Hazrati, 1995; Pasik et al., 1976). The few neurons with a notched or indented nucleus could be medium spiny projection neurons or could correspond to medium aspiny interneurons.

Labeled Terminals

In agreement with studies in monkey (DiFiglia et al., 1982) and most studies in rat (Bouyer et al, 1984a; Ingham et al., 1991; Roberts and Lapidus, 2003; Somogyi et al., 1982), axon terminals containing enkephalin immunoreactivity usually formed synapses with symmetric contacts. Axon terminals containing enkephalin labeling made symmetric synapses with both enkephalin-labeled and unlabeled profiles. Thus, from our data we can suggest that in humans, the medium spiny neurons of the indirect pathway not only modulate the activity of projection neurons within the direct pathway, but are able to modulate activity of the indirect pathway itself. This is consistent with results seen in other species (DiFiglia et al., 1982; Somogyi et al., 1982). A majority of the axon terminals positive for enkephalin in human striatum did not make any synaptic contact. This was verified by following the profile through its entirety in multiple planes of section, making this finding particularly interesting. This arrangement of labeled terminals is also present in rat striatum and has been suggested to be a nonsynaptic mechanism of interneuronal communication (Miller and Pickel, 1980). Other striatal afferents such as dopaminergic (Bouyer et al., 1984b; Kung et al., 1998; Pickel et al., 1981) and serotoninergic (Soghomonian et al., 1989) inputs also display non-junctional appositions, a finding that indicates that, in addition to acting through typical synaptic mechanisms, many striatal neuronal systems might also utilize volumic paracrine transmission as a mode of intercellular communication.

The larger density of labeled terminals forming symmetric synapses in the caudate nucleus compared to the putamen suggests that there are more local collaterals from enkephalin-containing neurons in the caudate nucleus than in the putamen. Labeled terminals forming asymmetric synapses were observed in the present study. This structural feature may vary between species, however the frequency in which it was observed was not usually quantified in studies of other species and is therefore difficult to compare (Table IV). Enkephalin-labeled terminals forming asymmetric synapses are rare in monkey (DiFiglia et al., 1982), and for the most part observed only occasionally in rat (Bouyer et al., 1984a; Ingham et al., 1991; Roberts and Lapidus, 2003; Somogyi et al., 1982). Only one study reported enkephalin-labeled terminals forming mostly asymmetric synapses, in rat (Pickel et al., 1980) and it has been suggested that this difference is due to differences in interpretation of synapse type (Somogyi et al., 1982) or the region observed (Bouyer et al., 1984a). While the density of labeled terminals forming asymmetric synapses was similar between the caudate and putamen, the proportion was greater in the putamen, due to fewer labeled terminals forming symmetric synapses in the putamen. However, it is important to note the small number of labeled terminals found in the putamen for quantification (Table II). Asymmetric synapses are usually regarded as a marker of excitatory transmission (Colonnier, 1968; Eccles, 1964; Landis et al., 1974), formed by terminals originating from cortex and thalamus, however, the source of enkephalin-labeled terminals forming asymmetric synapses is currently not known. Enkephalin has been shown to colocalize with 5-HT (serotonin) in cell bodies of the dorsal raphe nucleus (Glazer et al., 1981), a midbrain nucleus known to send serotoninergic projections to the dorsal striatum (Kitai, 1981; McQuade and Sharp, 1997; Steinbusch et al., 1981; Wallman et al., 2011) which form asymmetric synapses on dendritic spines and shafts of medium spiny neurons (Pasik et al., 1982; Soghomonian et al., 1989). Thus, it is possible that these enkephalin-labeled terminals forming asymmetric synapses could arise from the dorsal raphe nucleus. Regardless of the source, the similar density of labeled terminals forming asymmetric synapses in the two regions suggests the caudate nucleus and putamen are receiving similar representations of afferent innervation from enkephalin-containing neurons.

Enkephalin-positive terminals formed synapses with dendrites, spines, and cell bodies, while targeting dendrites and dendritic spines with similar frequencies. Interestingly, enkephalin-labeled terminals in the neuropil of rat and monkey primarily contact dendrites, while only

occasionally synapsing onto spines (DiFiglia et al., 1982; Ingham et al., 1991; Somogyi et al., 1982). Consistent with similar studies of striatal synaptic organization in human, terminals labeled with other markers, such as substance P and tyrosine hydroxylase, have also been reported to differ between human and other species. For example, terminals containing tyrosine hydroxylase tend to form axospinous synapses more frequently in human (65%; Kung et al., 1998) than in monkey (20%; Smith et al., 1994), and terminals containing substance P tend to form symmetric axospinous synapses more frequently in human (50%; Hutcherson and Roberts, 2005) than in rat (15%; Bolam and Izzo, 1988). The larger proportion of enkephalin-labeled terminals forming axospinous synapses was found in human as compared to both rodents and non-human primates, suggesting that this feature may be unique to humans. The significance of this finding is the implication that enkephalin has a more direct ability to modulate glutamatergic inputs in human striatum than in other species, which represents a departure in the human brain from that of other species.

Labeled Spine Morphology

The neuropil of the caudate nucleus and putamen were rich with enkephalin-labeled profiles receiving synapses. Among these labeled structures were dendritic spines conforming to several different morphologies. The functional significance of spine morphology has been studied theoretically and experimentally in regions throughout the brain. The structure of dendritic spines, including the shape and size of the spine head as well as the length of the spine neck, has been suggested to play a role in synaptic plasticity, long term potentiation (LTP), and the regulation of synaptic efficacy (for reviews see Calverley and Jones, 1990; Coss and Perkel, 1985; Harris and Kater, 1994). The volume of a spine head is proportional to the area of the postsynaptic density and to the number of presynaptic vesicles of the synapse (Arellano et al., 2007; Harris and Stevens, 1989; Schikorski and Stevens, 1999). Specifically, studies have shown that spines swell and shorten, and the area of the postsynaptic density increases with the induction of LTP (Chang and Greenough, 1984; Desmond and Levy, 1983, 1988; Van Harreveld and Fifkova, 1975). Additionally, studies on spine necks suggest their role in synaptic efficacy is by amplitude modulation (Perkel 1982-1983; Perkel and Perkel, 1985), and by the isolation of inputs electrically (Araya et al., 2006; Diamond et al., 1970; Jack et al., 1975; Llinás and Hillman, 1969) and biochemically (Denk et al., 1995; Majewska et al., 2000; Yuste and Denk, 1995; Yuste et al., 2000). The significance of spinules on spines has also been investigated and is suggested to play a role in remodeling of the dendritic spine or synapse (Calverley and Jones, 1990; Routtenberg and Tarrant, 1975). Due to the results of the present study which show that enkephalin labeling is present in spines of various morphologies, we suggest that enkephalin may play a role in the different types of plasticity discussed in the aforementioned studies. The difference in proportions of labeled spines between the caudate nucleus and the putamen may or may not reflect a physiological role in regard to plasticity of the two regions since the difference in proportion results from a lower density of total spines found in the putamen.

Perforated Synapses

Perforations in the postsynaptic density were observed in 25% of all axospinous synapses in human striatum. Axon terminals forming perforated synapses targeted labeled spines more frequently than unlabeled spines in putamen, whereas perforated synapses were more evenly distributed between labeled and unlabeled spines in the caudate nucleus. Interestingly, the opposite was found with substance P (Hutcherson and Roberts 2005), as would be expected since medium spiny neurons of the striatum contain either enkephalin or substance P, as discussed previously. Past studies investigating the origin and functionality of perforated synapses show that the axon terminals forming these synapses originate from cortex (Meshul et al., 1994; Meshul et al., 2000), and also show that these synapses play a morphological role in the enhancement of synaptic responsiveness (Geinisman et al.,

1986a,b, 1988, 1989; for review see Calverley and Jones, 1990). Thus, we can infer the significance of the differences between the prevalence of perforated synapses in the caudate nucleus and putamen. From the observation that a higher proportion of perforated synapses in the putamen target labeled spines and predominately, if not exclusively, labeled dendrites compared to perforated synapses in the caudate nucleus, it can be suggested that enkephalin-containing neurons in the putamen may play a larger role in cortical plasticity than those in the caudate nucleus. Moreover, perforated synapses have been associated with corticostriatal projections of the pyramidal tract (Reiner et al., 2003) which have been shown to preferentially target neurons of the indirect versus the direct pathway in rodents (Cepeda et al., 2008; Lei et al., 2004). If this is also true in humans, these data imply that enkephalinergic neurons of the putamen receive preferential input from the corticostriatal neurons of the pyramidal tract. Differences in synaptic organization between the caudate nucleus and the putamen have also been reported in human with substance P (Hutcherson and Roberts, 2005).

Enkephalin in the Pathophysiology of Basal Ganglia Disorders

Pathophysiology of the basal ganglia is implicated in motor disorders, such as Huntington's disease and Parkinson's disease (Albin et al., 1989; Penney and Young, 1983), as well as in non-motor psychiatric disorders (Calabresi et al., 1997). Enkephalin has been shown to be involved in a number of these disorders. For example, a marked decrease in enkephalin immunoreactivity is seen in the caudate-putamen, globus pallidus, and substantia nigra in patients of Huntington's disease and striatonigral degeneration (Albin et al., 1989; Ferrante et al., 1986; Goto et al., 1989; Marshall et al., 1983). Additionally, our laboratory (Roberts et al., 2005) has shown that patients with schizophrenia display an increase in asymmetric axospinous synapses in the caudate nucleus compared to normal controls, suggesting medium spiny neuron pathways in striatum play a role in the pathophysiology of schizophrenia. Being able to examine the synaptic localization in control human striatum is the first step in understanding the synaptic changes in medium spiny neuron pathways in diseases afflicting the basal ganglia, such as those listed above.

Acknowledgments

We would like to thank the members of the Maryland and Alabama Brain Collections and their associated entities for acquisition and preparation of human brains for electron microscopy. This work was supported by National Institutes of Health grant MH60744.

References

Albin RL, Young AB, Penney JB. The functional anatomy of basal ganglia disorders. Trends Neurosci. 1989; 12:366–375. [PubMed: 2479133]

Alexander GE, DeLong MR, Strick PL. Parallel organization of functionally segregated circuits linking basal ganglia and cortex. Ann Rev Neurosci. 1986; 9:357–381. [PubMed: 3085570]

Alexander GE, Crutcher MD, DeLong MR. Basal ganglia-thalamocortical circuits: parallel substrates for motor, oculomotor, 'prefrontal' and 'limbic' functions. Prog Brain Res. 1990; 85:119–146. [PubMed: 2094891]

Araya R, Jiang J, Eisenthal KB, Yuste R. The spine neck filters membrane potentials. Proc Natl Acad Sci USA. 2006; 103:18779–18804.

Arellano JI, Benavides-Piccione R, DeFelipe J, Yuste R. Ultrastructure of dendritic spines: correlation between synaptic and spine morphologies. Front Neurosci. 2007; 1:131–143. [PubMed: 18982124]

Aubert I, Ghorayeb I, Normand E, Bloch B. Phenotypical characterization of the neurons expressing the D1 and D2 dopamine receptors in monkey striatum. J Comp Neurol. 2000; 418:22–32. [PubMed: 10701753]

Beach TG, McGeer EG. The distribution of substance P in the primate basal ganglia: an immunohistochemical study of baboon and human brain. Neuroscience. 1984; 13:29–52. [PubMed: 6208509]

Beckstead RM, Kersey KS. Immunohistochemical demonstration of differential substance P-, met-enkephalin-, and glutamic-acid-decarboxylase-containing cell body and axon distributions in the corpus striatum of the cat. J Comp Neurol. 1985; 232:481–498. [PubMed: 2579980]

Björklund A, Dunnet SB. Dopamine neuron systems in the brain: an update. Trends Neurosci. 2007; 30:194–202. [PubMed: 17408759]

Bolam JP, Izzo PN. The postsynaptic targets of substance P-immunoreactive terminals in the rat neostriatum with particular reference to identified spiny striatonigral neurons. Exp Brain Res. 1988; 70:361–377. [PubMed: 2454839]

Bouyer JJ, Miller RJ, Pickel VM. Ultrastructural relation between cortical efferents and terminals containing enkephalin-like immunoreactivity in rat neostriatum. Requl Pept. 1984a; 8:105–115.

Bouyer JJ, Park DH, Joh TH, Pickel VM. Chemical and structural analysis of the relation between cortical inputs and tyrosine hydroxylase-containing terminals in rat neostriatum. Brain Res. 1984b; 302:267–275. [PubMed: 6145508]

Bryant, LA.; Roche, JK.; Roberts, RC. 491.14 2010 Neuroscience Meeting Planner. San Diego, CA: Society for Neuroscience; 2010. Immunocytochemical localization of enkephalin in the human striatum, a postmortem ultrastructural study.

Calabresi P, De Murtas M, Bernardi G. The neostriatum beyond the motor function: experimental and clinical evidence. Neuroscience. 1997; 78:39–60. [PubMed: 9135088]

Calverley RK, Jones DG. Contributions of dendritic spines and perforated synapses to synaptic plasticity. Brain Res Rev. 1990; 15:215–249. [PubMed: 2289086]

Cepeda C, André VM, Yamazaki I, Wu N, Kleiman-Weiner M, Levine MS. Differential electrophysiological properties of dopamine D1 and D2 receptor-containing striatal medium-sized spiny neurons. Eur J Neurosci. 2008; 27:671–682. [PubMed: 18279319]

Chang FLF, Greenough WT. Transient and enduring morphological correlates of synaptic activity and efficacy in the rat hippocampal slice. Brain Res. 1984; 309:35–46. [PubMed: 6488013]

Colonnier M. Synaptic patterns of different cell types in the different laminae of the cat visual cortex. An electron microscope study. Brain Res. 1968; 9:268–287. [PubMed: 4175993]

Coss RG, Perkel DH. The function of dendritic spines: a review of theoretical issues. Behav Neural Biol. 1985; 44:151–185. [PubMed: 2415102]

Denk W, Sugimori M, Llinás R. Two types of calcium response limited to single spines in cerebellar Purkinje cells. Proc Natl Acad Sci USA. 1995; 92:8279–8282. [PubMed: 7667282]

Desmond NL, Levy WB. Synaptic correlates of associative potentiation/depression: an ultrastructural study in the hippocampus. Brain Res. 1983; 265:21–30. [PubMed: 6850319]

Desmond NL, Levy WB. Synaptic interface surface area increases with long-term potentiation in the hippocampal dentate gyrus. Brain Res. 1988; 453:308–314. [PubMed: 3401768]

DiFiglia M, Aronin N, Martin JB. Light and electron microscopic localization of immunoreactive Leu-enkephalin in the monkey basal ganglia. J Neurosci. 1982; 3:303–320. [PubMed: 6121017]

DiFiglia M, Pasik T, Pasik P. A Golgi study of neuronal types in the neostriatum of monkeys. Brain Res. 1976; 114:245–256. [PubMed: 822916]

DiFiglia M, Pasik T, Pasik P. Ultrastructure of Golgi impregnated and gold-toned spiny and aspiny neurons in the monkey neostriatum. J Neurocytol. 1980; 9:471–492. [PubMed: 6160212]

Diamond, J.; Gray, EG.; Yasargil, GM. The function of dendritic spines: a hypothesis. In: Andersen, P.; Jansen, J., editors. Excitatory Mechanisms, Proceedings of 5th Internation Meeting of Neurobiologists. Oslo: Universitets Forlaget; 1970. p. 213-222.

Dubé L, Smith AD, Bolam JP. Identification of synaptic terminals of thalamic or cortical origin in contact with distinct medium-size spiny neurons in the rat neostriatum. J Comp Neurol. 1988; 267:455–471. [PubMed: 3346370]

Eccles, JC. The physiology of synapses. New York: Academic Press Inc; 1964.

Elde R, Hökfelt T, Johansson O, Terenius L. Immunohistochemical studies using antibodies to leucine-enkephalin: initial observations on the nervous system of the rat. Neuroscience. 1976; 1:349–351. [PubMed: 11370520]

Ferrante RJ, Kowall NW, Richardson EP Jr, Bird ED, Martin JB. Topography of enkephalin, substance P and acetylcholinesterase staining in Huntington's disease striatum. Neurosci Lett. 1986; 71:283–288. [PubMed: 2432445]

Frederickson RC, Norris FH. Enkephalin-induced depression of single neurons in brain areas with opiate receptors—antagonism by naloxone. Science. 1976; 194(4263):440–442. [PubMed: 10625]

Freund TF, Powell JF, Smith AD. Tyrosine hydroxylase-immunoreactive boutons in synaptic contact with identified striatonigral neurons, with particular reference to dendritic spines. Neuroscience. 1984; 13:1189–1215. [PubMed: 6152036]

Geinisman Y, de Toledo-Morrell L, Morrell F. Loss of perforated synapses in the dentate gyrus: morphological substrate of memory deficit in aged rates. Proc Natl Acad Sci USA. 1986a; 83:3027–3031. [PubMed: 3458260]

Geinisman Y, de Toledo-Morrell L, Morrell F. Aged rats need a preserved complement of perforated axospinous synapses per hippocampal neuron to maintain good spatial memory. Brain Res. 1986b; 389:266–275.

Geinisman Y, Morrell F, de Toledo-Morrell L. Remodeling of synaptic architecture during hippocampal "kindling". Proc Natl Acad Sci USA. 1988; 85:3260–3264. [PubMed: 2834740]

Geinisman Y, Morrell F, de Toledo-Morrell L. Perforated synapses on double-headed dendritic spines: a possible structural substrate of synaptic plasticity. Brain Res. 1989; 480:326–329. [PubMed: 2713659]

Geinisman Y, Gunderson HJG, Van Der Zee E, West MJ. Unbiased stereological estimation of the total number of synapses in a brain region. J Neurocytol. 1996; 12:805–819. [PubMed: 9023726]

Gerfen CR. Synaptic organization of the striatum. J Electron Microsc Tech. 1988; 10:265–281. [PubMed: 3069970]

Gerfen CR. The neostriatal mosaic: multiple levels of compartmental organization in the basal ganglia. Annu Rev Neurosci. 1992; 15:285–320. [PubMed: 1575444]

Gerfen CR, Engber TM, Mahan LC, Susel Z, Chase TN, Monsma FJ, Sibley DR. D1 and D2 dopamine receptor-regulated gene expression of striatonigral and striatopallidal neurons. Science. 1990; 250:1429–1432. [PubMed: 2147780]

Gerfen CR, McGinty JF, Young WS. Dopamine differentially regulates dynorphin, substance P, and enkephalin expression in striatal neurons: in situ hybridization histochemical analysis. J Neurosci. 1991; 11:1016–1031. [PubMed: 1707092]

Glazer EJ, Steinbusch H, Verhofstad A, Basbaum AI. Serotonin neurons in nucleus raphe dorsalis and paragigantocellularis of the cat contain enkephalin. J Physiol. 1981; 77:241–245.

Goto S, Hirano A, Rojas-Corona RR. Immunohistochemical visualization of afferent nerve terminals in human globus pallidus and its alteration in neostriatal neurodegenerative disorders. Acta Neuropathol. 1989; 78:543–550. [PubMed: 2479214]

Graveland AM, DiFiglia M. The frequency and distribution of medium-sized neurons with indented nuclei in the primate and rodent striatum. Brain Res. 1985; 327:307–311. [PubMed: 3986508]

Graybiel AM, Chesselet M. Compartmental distribution of striatal cell bodies expressing [Met]enkephalin-like immunoreactivity. Proc Natl Acad Sci USA. 1984; 81:7980–7984. [PubMed: 6440146]

Graybiel AM, Ragsdale CW, Yoneoka ES, Elde RP. An immunohistochemical study of enkephalins and other neuropeptides in the striatum of the cat with evidence that the opiate peptides are arranged to form mosaic patterns in register with the striosomal compartments visible by acetylcholinesterase staining. Neuroscience. 1981; 6:377–397. [PubMed: 6164013]

Groves PM, Martone M, Young SJ, Armstrong DM. Three-dimensional pattern of enkephalin-like immunoreactivity in the caudate nucleus of the cat. J Neurosci. 1988; 8:892–900. [PubMed: 3346727]

Haber SN. Neurotransmitters in the human and nonhuman primate basal ganglia. Hum Neurobiol. 1986; 5:159–168. [PubMed: 2876974]

Haber S, Elde R. The distribution of enkephalin immunoreactive fibers and terminals in the monkey central nervous system: an immunohistochemical study. Neuroscience. 1982; 7:1049–1095. [PubMed: 7050764]

Harris KM, Kater SB. Dendritic spines: cellular specializations imparting both stability and flexibility to synaptic function. Annu Rev Neurosci. 1994; 17:341–371. [PubMed: 8210179]

Harris KM, Stevens JK. Dendritic spines of CA1 pyramidal cells in the rat hippocampus: serial electron microscopy with reference to their biophysical characteristics. J Neurosci. 1989; 9:2982–2997. [PubMed: 2769375]

Henderson G, Hughes J, Kosterlitz HW. In vitro release of Leu- and Met-enkephalin from the corpus striatum. Nature. 1978; 271:677–679. [PubMed: 24181]

Hökfelt T, Elde R, Johansson D, Terrenius L, Stein L. The distribution of enkephalin-immunoreactive cell bodies in the rat central nervous system. Neurosci Lett. 1977; 5:25–31. [PubMed: 19604966]

Holt DJ, Graybiel AM, Saper CB. Neurochemical architecture of the human striatum. J Comp Neurol. 1997; 384:1–25. [PubMed: 9214537]

Hsu S, Raine L, Fanger H. Use of Avidin-Biotin-Peroxidase Complex (ABC) in immunoperoxidase techniques: a comparison between ABC and unlabeled antibody (PAP) procedures. J Histochem Cytochem. 1981; 29:577–580. [PubMed: 6166661]

Hughes J, Smith TW, Kosterlitz HW, Fothergill LA, Morgan BA, Morris HR. Identification of two related pentapeptides from the brain with potent opiate agonist activity. Nature. 1975; 258:577–580. [PubMed: 1207728]

Hutcherson L, Roberts RC. The immunocytochemical localization of substance P in the human striatum: a postmortem ultrastructural study. Synapse. 2005; 57:191–201. [PubMed: 15986364]

Ingaki S, Parent A. Distribution of enkephalin-immunoreactive neurons in the forebrain and upper brainstem of the squirrel monkey. Brain Res. 1985; 359:267–280. [PubMed: 3907752]

Jack, JJB.; Noble, D.; Tsien, RW. Electric current flow in excitable cells. London: Oxford University Press; 1975.

Kemp JM, Powell TPS. The structure of the caudate nucleus of the cat: light and electron microscopy. Phil Trans R Soc Lond. 1971a; 262:383–401. [PubMed: 4107495]

Kemp JM, Powell TPS. The synaptic organization of the caudate nucleus. Phil Trans R Soc Lond. 1971b; 262:403–412. [PubMed: 4399121]

Kemp JM, Powell TPS. The site of termination of afferent fibres in the caudate nucleus. Phil Trans R Soc Lond. 1971c; 262:413–427. [PubMed: 4399122]

Kitai ST. Anatomy and physiology of the neostriatum. Adv Biochem Psychopharmacol. 1981; 30:1–21. [PubMed: 6174034]

Kubota Y, Inagaki S, Kito S, Takagi H, Smith AD. Ultrastructural evidence of dopaminergic input to enkephalinergic neurons in rat neostriatum. Brain Res. 1986; 371:374–378. [PubMed: 2870770]

Kuhar MJ. Histochemical localization of opiate receptors and opioid peptides. Fed Proc. 1978; 37(2): 153–157. [PubMed: 203493]

Kung L, Force M, Chute DJ, Roberts RC. Immunocytochemical localization of tyrosine hydroxylase in the human striatum: a postmortem ultrastructural study. J Comp Neurol. 1998; 390:52–62. [PubMed: 9456175]

Landis DMD, Reese TS, Raviola E. Differences in membrane structure between excitatory and inhibitory components of the reciprocal synapse of the olfactory bulb. J Comp Neurol. 1974; 155:93–126. [PubMed: 4836065]

Lei W, Jiao Y, Del Mar N, Reiner A. Evidence for differential coritcal input to direct pathway versus indirect pathway striatal projection neurons in rats. J Neurosci. 2004; 24:8289–8299. [PubMed: 15385612]

Llinás, R.; Hillman, DE. Physiological and morphological organization of the cerebellar circuits in various vertebrates. In: Llinás, R., editor. Neurobiology of Cerebellar Evolution and Development. Chicago: Am Med Assoc Educ Res Found; 1969. p. 43-73.

Majewska A, Tashiro A, Yuste R. Regulation of spine calcium dynamics by rapid spine motility. J Neurosci. 2000; 20:8262–8268. [PubMed: 11069932]

Marshall PE, Landis DMD, Zalneraitis EL. Immunocytochemical studies of substance P and leucine-enkephalin in Huntington's disease. Brain Res. 1983; 289:11–26. [PubMed: 6198034]

Martin LJ, Hadfield MG, Dellovade TL, Price DL. The striatal mosaic in primates: patterns of neuropeptide immunoreactivity differentiate the ventral striatum from the dorsal striatum. Neuroscience. 1991; 43:397–417. [PubMed: 1681464]

Martone ME, Armstrong DM, Young SJ, Groves PM. Ultrastructural examination of enkephalin and substance P input to cholinergic neurons within the rat neostriatum. Brain Res. 1992; 594:253–262. [PubMed: 1280527]

McQuade R, Sharp T. Functional mapping of dorsal and median raphe 5-hydroxytyptamine pathways in forebrain of the rat using microdialysis. J Neurochem. 69:791–796. [PubMed: 9231740]

Meshul CK, Cogen JP, Cheng H, Moore C, Krentz L. Alterations in rat striatal glutamate synapses following a lesion of the cortico- and/or nigrostriatal pathway. Exp Neurol. 2000; 165:191–206. [PubMed: 10964498]

Meshul CK, Stallbaumer RK, Taylor B, Janowsky A. Haloperidol-induced morphological changes in striatum are associated with glutamate synapses. Brain Res. 1994; 648:181–195. [PubMed: 7922533]

Miller RJ, Pickel VM. The distribution and functions of enkephalins. J Histochem and Cytochem. 1980; 28:903–917. [PubMed: 7003009]

Parent A, Hazrati LN. Functional anatomy of the basal ganglia. I. The cortico-basal ganglia-thalamo-cortical loop. Brain Res Rev. 1995; 20:91–127. [PubMed: 7711769]

Pasik P, Pasik T, DiFiglia M. Quantitative aspects of neuronal organization in the neostriatum of the macaque monkey. Res Publ Assoc Res Nerv Ment Dis. 1976; 55:57–90. [PubMed: 827000]

Pasik, P.; Pasik, T.; DiFiglia, M. The internal organization of the neostriatum in mammals. In: Divac, I.; Orberg, RGE., editors. The Neostriatum. Oxford: Pergamon Press; 1979. p. 5-36.

Pasik P, Pasik T, Saavedra JP. Immunocytochemical localization of serotonin at the ultrastructural level. J Histochem Cytochem. 1982; 30:760–764. [PubMed: 6181120]

Pasternak GW, Simantov R, Snyder SH. Characterization of endogenous morphine-like factor (enkephalin) in mammalian brain. Mol Pharmacol. 1975; 12:504–513. [PubMed: 934061]

Penney JB, Young AB. Speculation on the functional anatomy of basal ganglia disorders. Ann Rev Neurosci. 1983; 6:73–94. [PubMed: 6838141]

Penny GR, Afsharpour S, Kitai ST. The glutamate decarboxylase-, leucine enkephalin-, methionine enkephalin- and substance P-immunoreactive neurons in the neostriatum of the rat and cat: evidence for partial population overlap. Neuroscience. 1986; 17:1011–1045. [PubMed: 2423919]

Perez-Costas E, Melendez-Ferro M, Roberts RC. Microscopy techniques and the study of synapses. Modern Research and Educational Topics in Microscopy. 2007; 1:164–170.

Perez-Costas E, Melendez-Ferro M, Roberts RC. Basal ganglia pathology in schizophrenia: dopamine connections and anomalies. J Neurochem. 2010; 113:287–302. [PubMed: 20089137]

Perkel DH. Functional role of dendritic spines. J Physiol. 1982-1983; 78:695–699.

Perkel DH, Perkel DJ. Dendritic spines: role of active membrane in modulating synaptic efficacy. Brain Res. 1985; 325:331–335. [PubMed: 2579708]

Pickel VM, Beckley SC, Joh TH, Reis DJ. Ultrastructural immunocytochemical localization of tyrosine hydroxylase in the neostriatum. Brain Res. 1981; 225:373–385. [PubMed: 6118197]

Pickel VM, Sumai KK, Beady SC, Miller RJ, Reis DJ. Immunocytochemical localization of enkephalin in the neostriatum of rat brain: a light and electron microscopic study. J Comp Neurol. 1980; 189:721–740. [PubMed: 6991552]

Prensa L, Giménez-Amaya JM, Parent A. Chemical heterogeneity of the striosomal compartment in the human striatum. J Comp Neurol. 1999; 4:603–618. [PubMed: 10495446]

Reiner A, Jiao Y, Del Mar N, Laverghetta AV, Lei WL. Differential morphology of pyramidal tract-type and intratelencephalically projecting-type corticostriatal neurons and their intrastriatal terminals in rats. J Comp Neurol. 2003; 457:420–440. [PubMed: 12561080]

Roberts RC, Knickman JK. The ultrastructural organization of the patch matrix compartments in the human striatum. J Comp Neurol. 2002; 452:128–138. [PubMed: 12271487]

Roberts RC, Lapidus B. Ultrastructural correlates of haloperidol-induced oral dyskinesias in rats: a study of unlabeled and enkephalin-labeled striatal terminals. J Neural Transm. 2003; 110:961–975. [PubMed: 12938022]

Roberts RC, Roche JK, Conley RR. Synaptic differences in the postmortem striatum of subjects with schizophrenia: a stereological ultrastructural analysis. Synapse. 2005; 56:185–197. [PubMed: 15803499]

Routtenberg A, Tarrant S. The extended spinule complex: dendritic spine invagination of presynaptic terminals. Anat Rec. 1975; 181:467–473.

Sar M, Stumpf WE, Miller RJ, Chang KJ, Cuatrecasas P. Immunohistochemical localization of enkephalin in rat brain and spinal cord. J Comp Neurol. 1978; 182:17–38. [PubMed: 359601]

Schikorski T, Stevens C. Quantitative fine-structural analysis of olfactory cortical synapses. Proc Natl Acad Sci USA. 1999; 96:4107–4112. [PubMed: 10097171]

Simantov R, Kuhar MJ, Uhl GR, Snyder SH. Opioid peptide enkephalin: immunohistochemical mapping in rat central nervous system. Proc Natl Acad Sci USA. 1977; 74:2167–2171. [PubMed: 194249]

Smith Y, Bennett BD, Bolam JP, Parent A, Sadikot AF. Synaptic relationships between dopaminergic afferents and cortical or thalamic input in the sensorimotor territory of the striatum in monkey. J Comp Neurol. 1994; 344:1–19. [PubMed: 7914894]

Smith Y, Bevan MD, Shink E, Bolam JP. Microcircuitry of the direct and indirect pathways of the basal ganglia. Neuroscience. 1998; 86:353–387. [PubMed: 9881853]

Soghomonian JJ, Descarries L, Watkins KC. Serotonin innervation in adult rat neostriatum. II. Ultrastructural features: a radiographic and immunocytochemical study. Brain Res. 1989; 481:67–86. [PubMed: 2706468]

Somogyi P, Priestley JV, Cuello AC, Takagi H. Synaptic connections of enkephalin-immunoreactive nerve terminals in the neostriatum: a correlated light and electron microscopic study. J Neurocytol. 1982; 11:779–807. [PubMed: 6754878]

Steinbusch HW, Nieuwenhuys R, Verhofstad AA, Van der Kooy D. The nucleus raphe dorsalis of the rat and its projection upon the caudatoputamen. A combined cytoarchitectonic, immunohistochemical and retrograde transport study. J Physiol. 1981; 77:157–174.

Sterio DC. The unbiased estimation of number and size of arbitrary particles using the dissector. J Microsc. 1984; 134:127–136. [PubMed: 6737468]

Tepper JM, Abercrombie ED, Bolam JP. Basal ganglia macrocircuits. Prog Brain Res. 2007; 160:1–7.

Tripathi A, Prensa L, Cebrián C, Mengual E. Axonal branching patterns of nucleus accumbens neurons in the rat. J Comp Neurol. 2010; 518:4649–4673. [PubMed: 20886627]

Van Harreveld A, Fifkova E. Swelling of dendritic spines in the fascia dentate after stimulation of the perforant fibers as a mechanism of post-tetanic potentiation. Exp Neurol. 1975; 49:736–749. [PubMed: 173566]

Wallman MJ, Gagnon D, Parent M. Serotonin innervation of human basal ganglia. Eur J Neurosci. 2011; 33:1519–1532. [PubMed: 21375599]

Yung KK, Smith ED, Levey AI, Bolam JP. Synaptic connections between spiny neurons of the direct and indirect pathways in the neostriatum of the rat: evidence from dopamine receptor and neuropeptide immunostaining. Eur J Neurosci. 1996; 8:861–869. [PubMed: 8743734]

Yuste R, Denk W. Dendritic spines as basic units of synaptic integration. Nature. 1995; 375:682–684. [PubMed: 7791901]

Yuste R, Majewska A, Holthoff K. From form to function: Calcium compartmentalization in dendritic spines. Nat Neurosci. 2000; 3:653–659. [PubMed: 10862697]

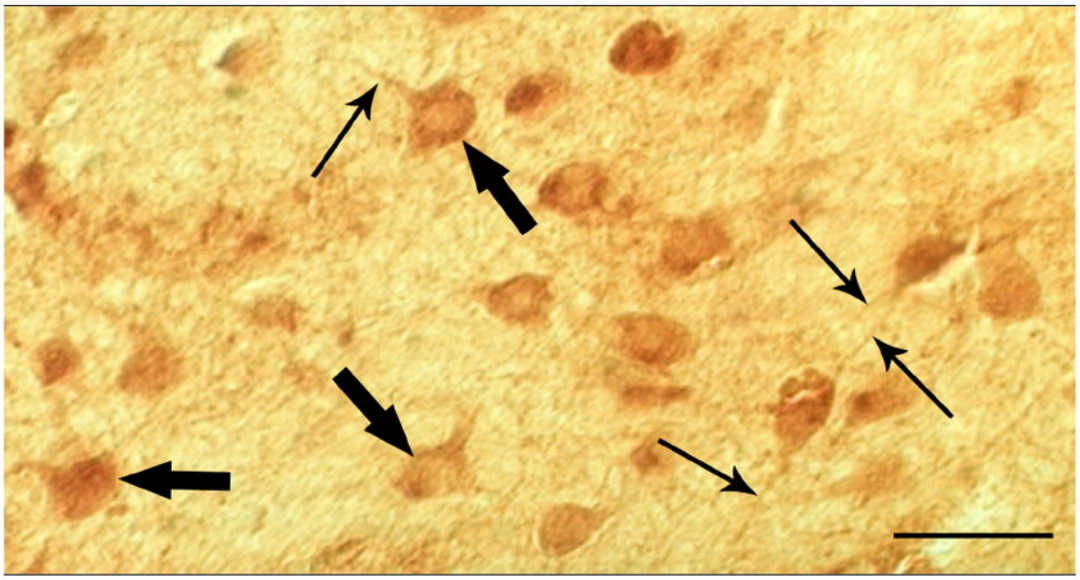

Figure 1.
Light micrograph taken at 40X of enkephalin-labeled neurons in human striatum. Medium-sized neurons are labeled (large arrows) as well as processes (small arrows). Scale bar, 50 μm.

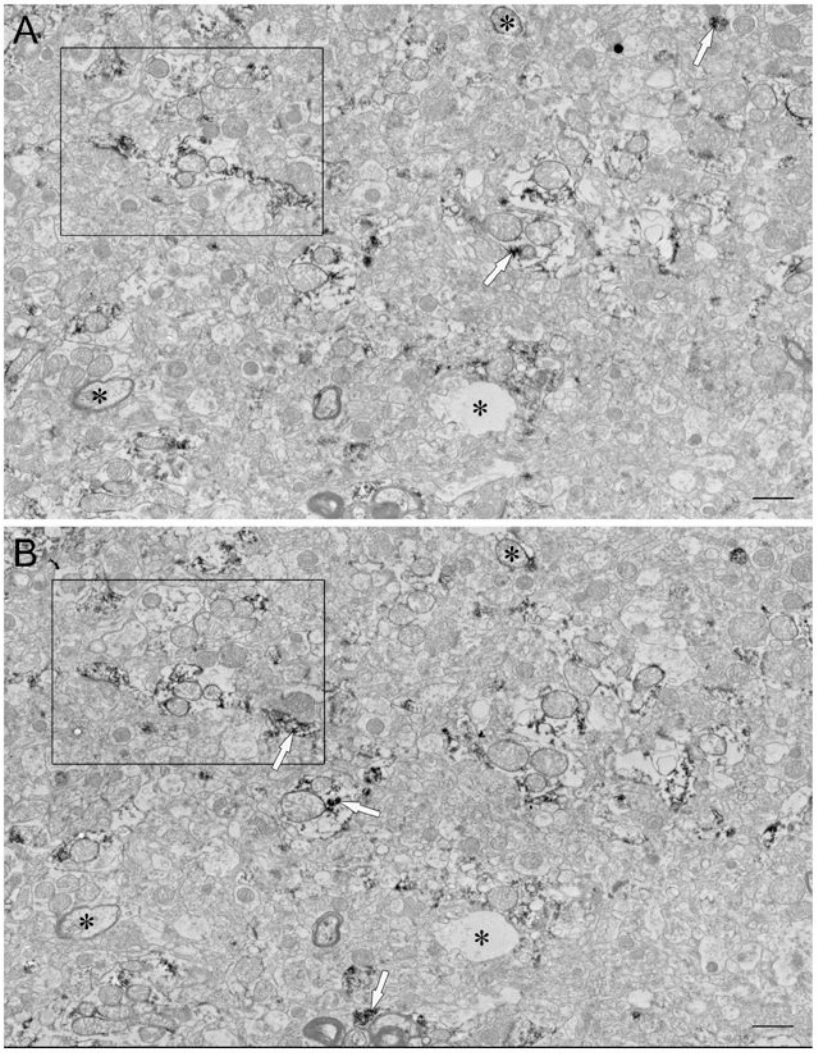

Figure 2.

Representative subsections of neuropil montages used for stereology, constructed from 8 individual micrographs. **(A)** and **(B)** are adjacent serial sections in a ribbon of 16 sections from the caudate nucleus of case #M3. Distinguishable structures (asterisks) are used to locate the same area in each serial section. See Fig. 2 for higher magnification of area in rectangles. Reaction product is indicated by white arrows. Scale bars, 1 μm.

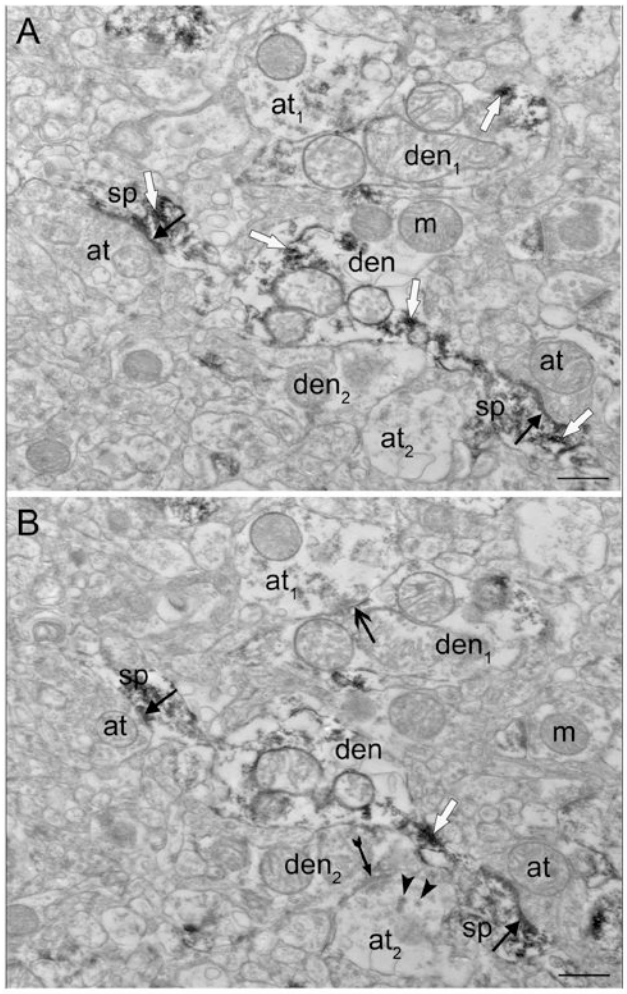

Figure 3.

Higher magnification of nearby serial sections of area in rectangles in Fig. 1. (**A**) Two labeled spines (sp) emerging from the same dendrite (den) receive asymmetric synapses (closed black arrows) from unlabeled axon terminals (at). Synapses are also present in **B**. (**B**) A new symmetric synapse (open black arrow) appears between a lightly labeled terminal (at_1) and a lightly labeled dendrite (den_1). Dense core vesicles (arrowheads) are present in an unlabeled axon terminal (at_2) which forms a new asymmetric synapse (closed black arrow with tail) with an unlabeled dendrite (den_2). Reaction product is indicated by white arrows. Scale bars, 0.5 μm.

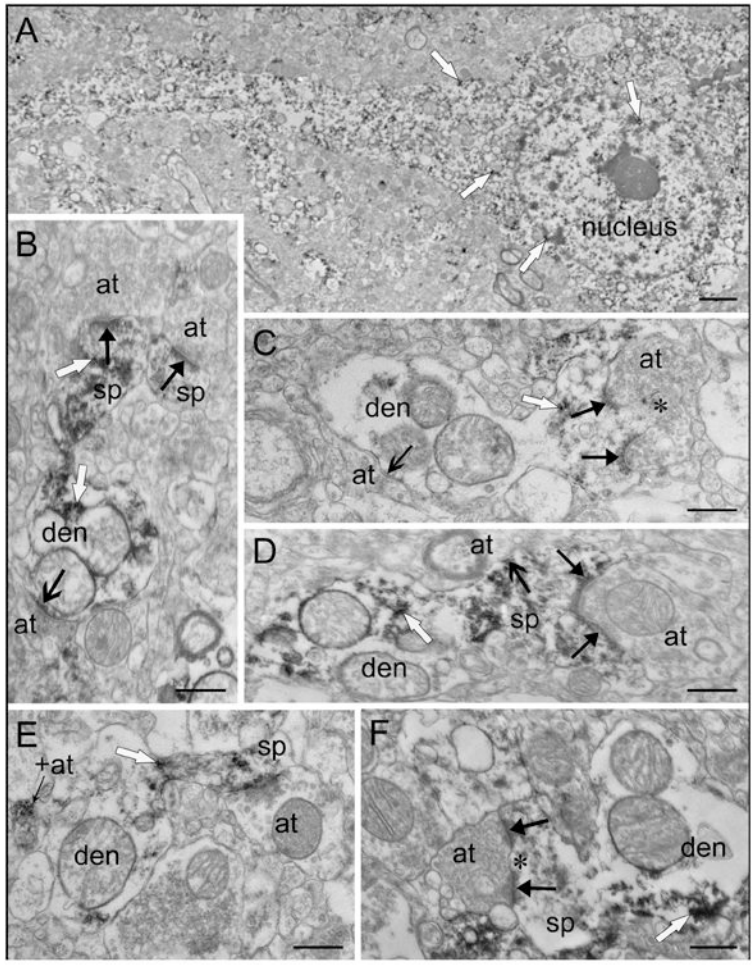

Figure 4.

Medium spiny neuron and spine morphology. (**A**) A medium spiny neuron contains small clusters of enkephalin immunoreactivity throughout the perikarya, dendrite, and nucleus. (**B**) A labeled spine (sp) with a large head and thin neck emerges from a labeled dendrite (den), and receives an asymmetric synapse (solid black arrow). An adjacent labeled spine head also receives an asymmetric synapse (solid black arrow). Note the symmetric axodendritic synapse (open arrow). All three axon terminals (at) are unlabeled. (**C**) A spine with a spinule (asterisk) emerges from a dendrite (den). The spine is lightly labeled and receives a perforated asymmetric synapse (solid black arrows) from an unlabeled terminal (at). The dendrite receives a symmetric synapse (open black arrow) from an unlabeled terminal (at). (**D**) A labeled spine (sp) with a large head and wide neck emerges from a dendrite (den) and receives an asymmetric synapse (solid black arrows) and a symmetric synapse (open black arrow) from unlabeled axon terminals (at). (**E**) A labeled spine (sp) with a thin neck and head emerges from a dendrite. An unlabeled terminal (at) makes contact with the spine head but does not meet all three synaptic criteria since a clear synaptic cleft is not present. A nearby labeled axon terminal (+at) is adjacent to the dendrite but does not form a synapse. (**F**) A mushroom shaped spine (sp) emerges from a labeled dendrite (den). An unlabeled axon terminal makes a perforated (asterisk) asymmetric synapse (solid black arrows). Reaction product is indicated by white arrows. Scale bars: **A**, 2 μm; **B-F**, 0.5 μm.

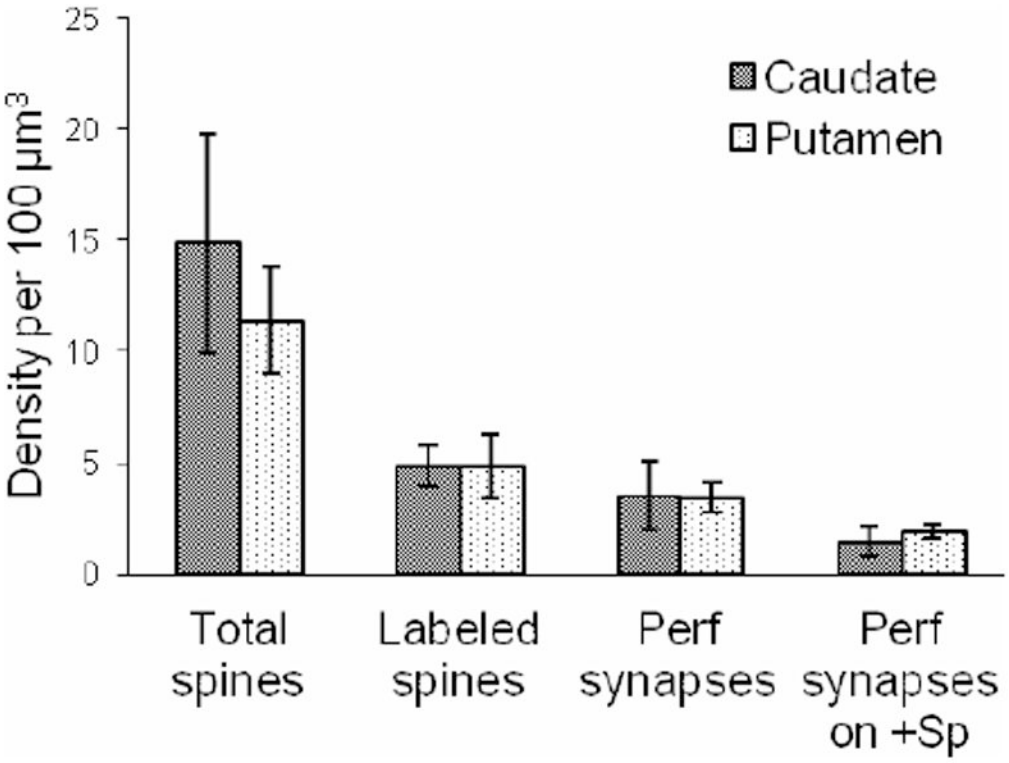

Figure 5.
Density (per 100 μm^3) of synapses formed on spines (total spines; labeled and unlabeled), synapses formed on labeled spines (+Sp), perforated (perf) synapses, and perforated synapses on labeled spines in the caudate and putamen. Densities were averaged over cases. Error bars, standard deviation.

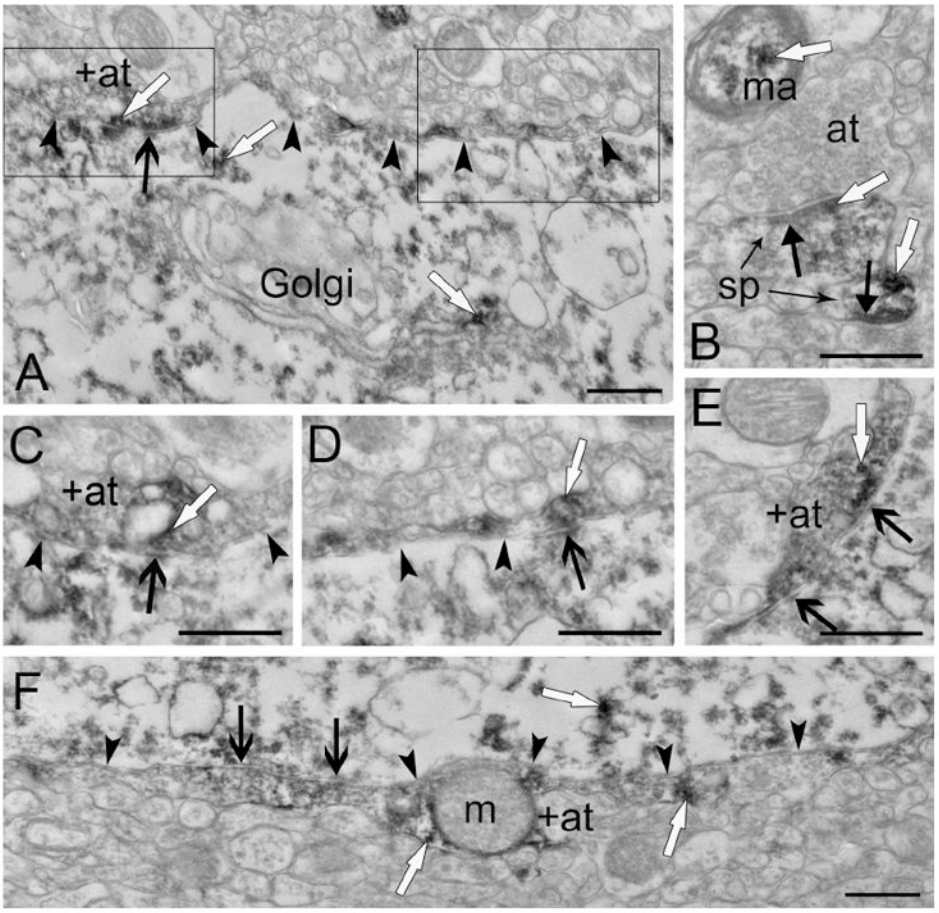

Figure 6.

(**A**) A long, labeled axon terminal (+at, arrowheads) makes a symmetric synapse (open black arrow) with a labeled cell body. Serial sections of the labeled terminal, shown in **C**-**E**, show the terminal forming multiple symmetric synapses with the soma. The portion of the labeled terminal in the left rectangle is shown in **C** and **E**. The portion of the labeled terminal in the right rectangle is shown in **D**. (**B**) Nearby neuropil contains a myelinated axon (ma) with enkephalin labeling and two labeled spines (sp) each receiving an asymmetric synapse (closed black arrows) from unlabeled axon terminals (at). (**C**) A higher magnification serial section of the area in the left rectangle of **A**. The labeled axon terminal (+at) makes a symmetric synapse (open black arrow) with the soma. (**D**) A higher magnification serial section of the area in the right rectangle of **A** shows the labeled axon terminal (arrowheads) making another symmetric synapse (open black arrow) with the soma. (**E**) Another higher magnification serial section of the area in the left rectangle of **A**. The labeled axon terminal (+at, arrowheads) makes multiple symmetric synapses (open black arrows) with the soma. (**F**) Another long labeled terminal (+at, arrowheads) making multiple symmetric synapses (open black arrows) with a labeled cell body. Reaction product is indicated by white arrows. Scale bars, 0.5 μm.

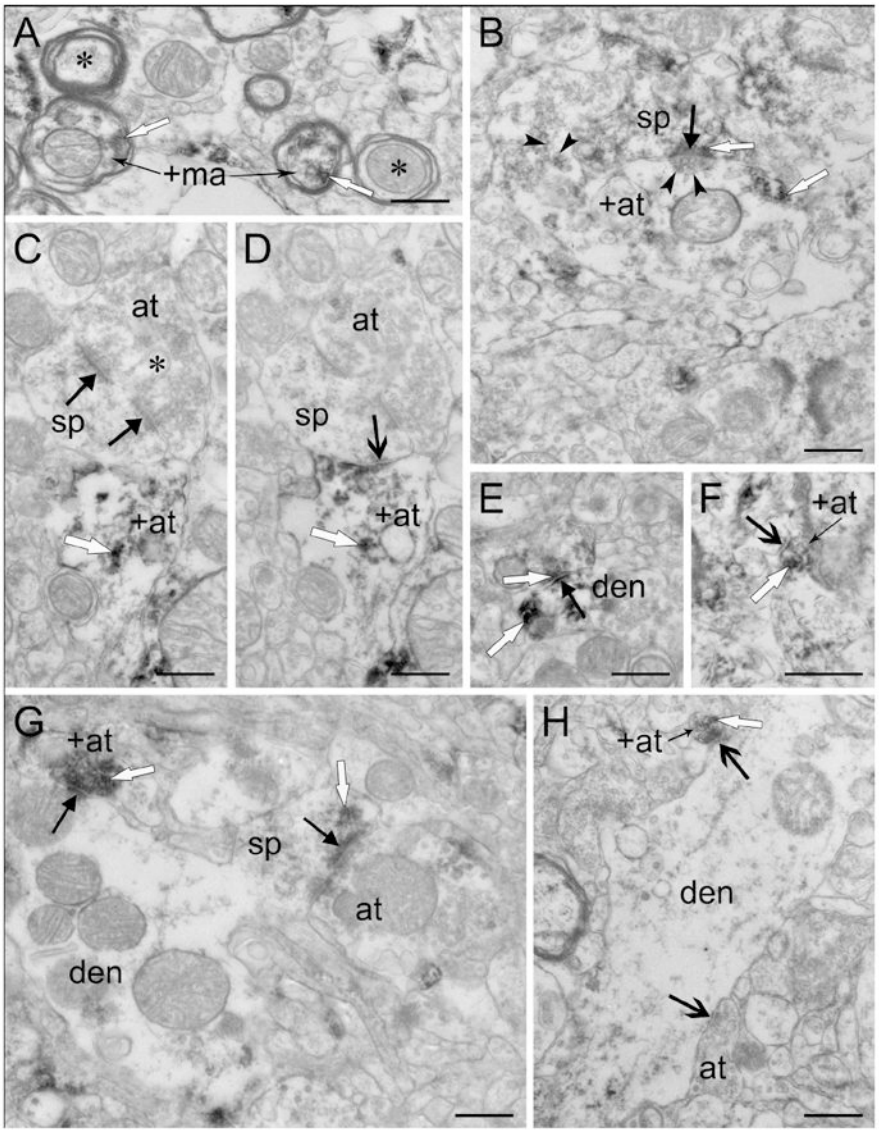

Figure 7.

Labeled axon terminals making synapses on labeled and unlabeled profiles. (**A**) Myelinated axons containing enkephalin immunoreactivity (+ma). Note nearby unlabeled myelinated axons (asterisks). (**B**) A large, lightly labeled axon terminal (+at) makes an asymmetric synapse (solid black arrow) with a labeled spine (sp). Round clear vesicles (arrowheads) are indicated. **(C-D)** Adjacent serial micrographs of an unlabeled spine (sp) with a spinule (asterisk) receiving multiple synapses. An unlabeled axon terminal (at) makes an asymmetric perforated synapse (solid black arrows) with the spine in **C**, also present in **D**. A symmetric axospinous synapse (open black arrow) formed by a labeled axon terminal (+at) appears in **D**. (**E**) A lightly labeled axon terminal makes an asymmetric synapse (solid black arrow), as identified in serial sections, with a labeled dendrite (den). (**F**) A labeled axon terminal (+at) makes a symmetric synapse (open black arrow) with an unlabeled spine neck. (**G**) A dendrite (den) receives an asymmetric synapse (solid black arrow) from a labeled axon terminal (+at). Also, a lightly labeled spine (sp) emerging from the dendrite receives an asymmetric synapse (solid black arrow) from an unlabeled terminal (at). (**H**) A labeled axon

terminal (+at) makes a symmetric synapse with an unlabeled dendrite (den). Note the symmetric axodendritic synapse (open black arrow) made by an unlabeled terminal (at). Reaction product is indicated by white arrows. Scale bars, 0.5 μm.

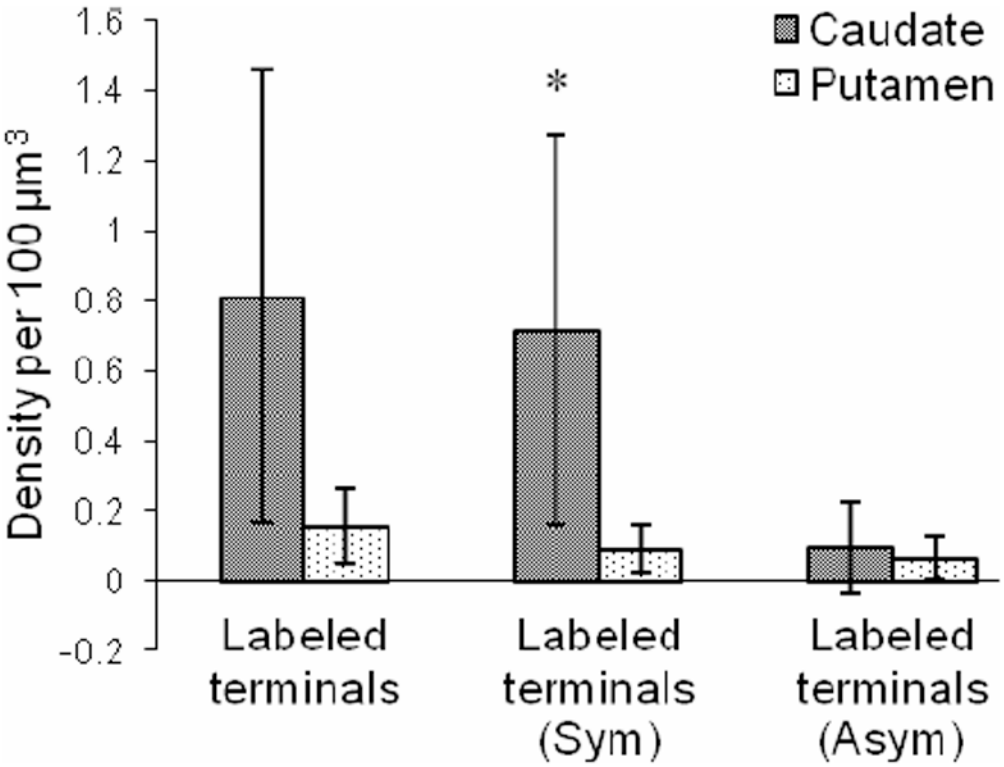

Figure 8.
Density (per 100 μm^3) of all labeled terminals making synapses, labeled terminals forming symmetric synapses (Sym) and labeled terminals forming asymmetric synapses (Asym) in the caudate and putamen. Densities were averaged over cases. Error bars, standard deviation. *, $P < 0.05$.

Synapse. Author manuscript; available in PMC 2013 March 01.

Table I

Demographics of postmortem cases.

Case	A/R/G[1]	PMI[2]	pH	Cause of death[3]	ABC/MBC
M1	47CM	6	6.60	ASCVD	MBC
M2	68AM	5	7.14	ASCVD	MBC
M3	32CF	7	7.00	Cardiac arrhythmia	MBC
M5	48AM	3	n/a	MVA	MBC
M7	43AF	6	7.18	ASCVD	MBC
A8*	68CM	7	6.20	Cardiac arrest	ABC
A9*	67CM	8	6.60	Lung cancer	ABC
A10*	32CF	8	6.30	Cardiac arrest	ABC

Case history for postmortem human brains obtained from the Alabama Brain Collection (ABC) and Maryland Brain collection (MBC) used for qualitative and quantitative analyses of enkephalin localization in human striatum.

[1] A/R/G, age(years)/race/gender; A, African-American; C, Caucasian; F, female; M, male.

[2] PMI, postmortem interval (hours).

[3] ASCVD, atherosclerotic cardiovascular disease; MVA, motor vehicle accident.

* Cases were observed but not quantified.

Table II

Quantitative data and proportions.

	Stereology			SPC
	Caudate	**Putamen**	**C+P**	**C+P**
Synapses formed on labeled (+) spines				
# + spines/total spines	239/751	408/929	647/1680	
% + spines	32%	44%	39%	
Labeled axon terminals (+AT)				
# + AT/total axon terminals	37/859	12/1127	49/1986	
% + AT	4%	1%	2%	
+AT synapsing on spines and dendrites[1]				
# + AT synapsing on spines (sp)	18	7	25	17
# + AT synapsing on dendrites (den)	19	5	24	15
% + AT synapsing on sp vs den	49%	58%	51%	53%
+AT making sym vs asym synapses[2]				
AS, AD	3, 1	3, 2	6, 3	5, 1
SS, SD	15, 18	4, 3	19, 21	12, 14
% + AT forming symmetric synapses	89%	58%	82%	81%
+AT synapsing on neg vs + profiles[3]				
# + AT on + profiles (sp,den)	4 (2,2)	3 (1,2)	7 (3,4)	7 (4,3)
# + AT on neg profiles (sp,den)	33 (16,17)	9 (6,3)	42 (22,20)	25 (13,12)
% + AT on +profiles	11%	25%	14%	22%
Spines (sp) with perf psds[4]				
% of all sp with perf psds	20%	29%	25%	
% of perf psds on + vs neg sp	47%	59%	55%	
% of + sp w/perf psds vs all + sp	26%	39%	34%	
% of neg sp w/perf psds vs all neg sp	16%	21%	19%	

Results of the quantitative analysis of the number (#) and percentage (%) of labeled (+) and unlabeled (neg) profiles counted using stereology and simple profile counts (SPC) from the caudate nucleus, the putamen, and the combined totals (C+P).

[1] Labeled axon terminals (+AT) forming synapses on spines and dendrites.

[2] Labeled axon terminals (+AT) forming symmetric (sym) vs. asymmetric (asym) synapses. AS, asymmetric axospinous; AD, asymmetric axodendritic; SS, symmetric axospinous; SD, symmetric axodendritic.

[3] Labeled axon terminals (+AT) forming synapses on labeled (+) spines or dendrites (sp,den), or on unlabeled (neg) spines or dendrites (sp,den).

[4] Percentage (%) of labeled (+) and unlabeled (neg) spines (sp) that possessed synapses with perforated postsynaptic densities (perf psds).

Table III

Caudate-putamen comparison

	Caudate	Putamen	*p*
+Spines	4.99±1.22	4.92±1.11	0.686
Neg spines	9.91±3.95	6.49±1.65	0.138
+PSS	5.28±1.21	5.72±0.99	0.416
+Sp w/ perf psd	1.47±0.68	1.91±0.33	0.080
+AT	0.81±0.65	0.16±0.11	0.080
+AT (sym)	0.72±0.55	0.09±0.07	0.043
+AT (asym)	0.10±0.13	0.07±0.06	0.465
+AT (neg PSS)	0.36±0.01	0.06±0.02	0.043
+AT (+ PSS)	0.09±0.18	0.04±0.08	0.593

The mean±SD of density data (100 μm^3) for all 5 individuals quantified. Variability for only salient data is shown: labeled and unlabeled spines receiving synapses (+Spines, Neg spines), synapses on labeled postsynaptic structures (+PSS; dendrites and spines), labeled spines with perforated postsynaptic densities (+Sp w/ perf psd), labeled axon terminals (+AT) making symmetric (sym) or asymmetric (asym) synapses and labeled axon terminals synapsing with unlabeled (neg PSS) or labeled (+PSS) postsynaptic structures. *P* values shown are comparing caudate and putamen (n=5).

Table IV

Comparison of enkephalin-labeled axon terminals among species.

	Rat				Monkey	Human
	Pickel et al. 1980	**Somogyi et al. 1982**	**Bouyer et al. 1984**	**Ingham et al. 1991**	**DiFiglia et al. 1982**	**Present study**
PSD symmetry[1]						
Symmetric	Absent	Most	Most	92%	Most	82%
Asymmetric	Most	Rare	Few	8%	Rare	18%
Dendritic Targets[2]						
Axospinous	NA	Rare	NA	18%	Rare	51%
Axodendritic	NA	Common	NA	67%	Most	49%
Other contacts						
Axosomatic[3]	Present/neg	Present/neg	NA	6.5%	Present/+	Present/+
Axoaxonic[4]	Syn (AT)	DA	DA	NA	Syn (IS)	DA
With + profiles[5]	Absent	NA	NA	NA	Present	Present

Data based on qualitative reports and quantitative reports (when provided) of enkephalin-labeled terminals. NA, data not available.

[1] Symmetry of the postsynaptic density (PSD).

[2] Comparison of whether synapses onto dendrites targeted spines or the dendrite shaft. Studies where data are not available did not qualitatively or quantitatively distinguish between synapses on spines and shafts.

[3] Observation of a labeled synapse onto an unlabeled (neg) or labeled (+) cell body.

[4] Studies that reported labeled terminals forming synapses (Syn) with other axons, or reported a labeled terminal in direct apposition (DA) to another axon but no membrane specialization present. AT, axoaxonic synapses formed another axon terminal; IS, axoaxonic synapses formed with axon hillock or initial segments. All direct appositions were with other axon terminals.

[5] Labeled terminals forming a synapse with a labeled (+) postsynaptic profile.